Theoretical Studies of the Coordination and Stability of Divalent Cations in ZSM-5

Mark J. Rice,[†] Arup K. Chakraborty,[†,‡] and Alexis T. Bell*[,†]

Chemical and Materials Sciences Divisions, Lawrence Berkeley National Laboratory, Departments of Chemical Engineering and Chemistry, University of California, Berkeley, California 94720-1462

Received: March 13, 2000; In Final Form: August 20, 2000

The coordination of divalent metal cations to ZSM-5 has been investigated using gradient-corrected density functional theory (DFT). Coordination at both isolated charge-exchange sites and pairs of charge-exchange sites was considered for Co^{2+}, Cu^{2+}, Fe^{2+}, Ni^{2+}, Pd^{2+}, Pt^{2+}, Ru^{2+}, Rh^{2+}, and Zn^{2+}. Thermodynamic calculations of the stability of M^{2+} to reduction to M^0 and demetalation to form MO_x particles were also carried out. The results indicate that Cu^{2+}, Co^{2+}, Fe^{2+}, and Ni^{2+} are coordinated preferentially to five-membered rings containing two Al atoms, which are located on the walls of the sinusoidal channels, whereas Pd^{2+}, Pt^{2+}, Ru^{2+}, Rh^{2+}, and Zn^{2+} are coordinated preferentially to six-membered rings located on the walls of the sinusoidal channels. Examination of the stability of dimer cations of the form $[M-O-M]^{2+}$ shows that such structures are not generally stable to hydrolysis, with the possible exception of $[Cu-O-Cu]^{2+}$. The findings of these calculations are in good general agreement with experimental results.

Introduction

The exchange of group VIII and other metals into the zeolite ZSM-5 produces materials that exhibit catalytic activity for NO decomposition,[1−5] N_2O decomposition,[6−10] selective catalytic reduction of NO by ammonia and light hydrocarbons,[11−22] and aromatization of hydrocarbons.[23,24] Extended X-ray absorption fine structure (EXAFS), X-ray absorption near edge structure (XANES), and UV−vis studies of metal-exchanged ZSM-5 indicate that divalent cations, M^{2+}, can be associated with either one or two charge-exchange sites in the zeolite. The first of these cases is represented by $Z^-[M(OH)]^+$, where Z^- designates a charge-exchange site. When two Al charge-exchange sites are in proximity, such as in rings containing four, five, or six T sites, structures of the type $Z^-M^{2+}Z^-$ can be formed. There is also a growing body of evidence suggesting the presence of dimer cations in which two M^{2+} cations are bridged by an O atom or two M^{3+} cations are bridged by two O atoms.[21−35] Such structures can be represented by $Z^-[M(O)M]^{2+}Z^-$ and $Z^-[M(O)_2M]^{2+}Z^-$. The experimental evidence also indicates that M^{2+} cations can be reduced to form small metal particles or can react with oxygen and water to form metal oxide particles. Occurrence of either of these processes generally leads to a loss in catalytic activity and selectivity.[36,37] For these reasons, it is desirable to understand the relative stability of M^{2+} cations in ZSM-5 as a function of cation composition and location of the charge-exchange site in the zeolite. A closely related question is whether the formation of dimer cations is thermodynamically favorable, as has been suggested by recent quantum chemical calculations.[38,39] In the present study, density functional theory (DFT) is used to determine the structure of Co^{2+}, Cu^{2+}, Fe^{2+}, Ni^{2+}, Pd^{2+}, Pt^{2+}, Rh^{2+}, Ru^{2+}, and Zn^{2+} exchanged into ZSM-5. The energy of cation reduction and demetalation is also determined from DFT calculations, whereas the entropy of reaction for each of these processes is determined with additional statistical mechanics calculations. Taken together, these calculations enable one to determine the relative stability of M^{2+} cations in different charge-exchange sites and the stability of the cation with respect to reduction and demetalation.

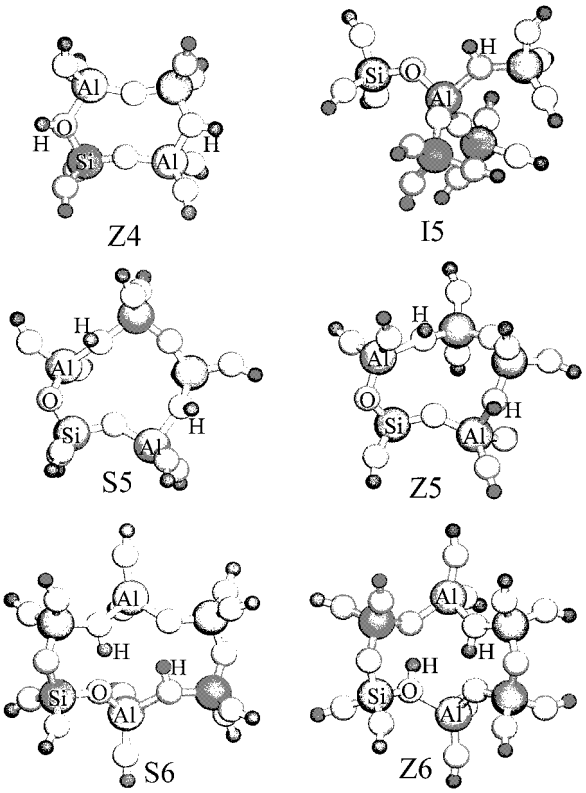

Figure 1. Structures of I5, Z4, S5, Z5, S6, and Z6 clusters in their acidic form.

Theoretical Methods

The zeolite is represented by a cluster containing between 4 and 6 T sites (Si or Al) and between 25 and 39 atoms in total. Figure 1 illustrates the structure of these clusters in their

[†] Department of Chemical Engineering.
[‡] Department of Chemistry.

10.1021/jp0009352 CCC: $19.00
Published on Web 10/05/2000

TABLE 1: Cluster Classification and Identification

cluster label	type	location	T sites	Al positions
Z4	ring	zigzag	T9 T9 T10 T10	T9 T10
S5	ring	straight	T3 T5 T6 T11 T12	T6 T11
I5	branched	intersection	T3 T8 T11 T12 T12	T12
Z5	ring	zigzag	T3 T4 T7 T8 T12	T8 T12
S6	ring	straight	T7 T7 T11 T11 T12 T12	T11 T11
Z6	ring	zigzag	T7 T7 T10 T10 T11 T11	T11 T11
SZ8	multiple rings	straight/zigzag	T7 T7 T10 T10 T11 T11 T12 T12	T11 T11
I9	branched	intersection	T2 T3 T3 T4 T6 T8 T11 T12 T12	T3 T12

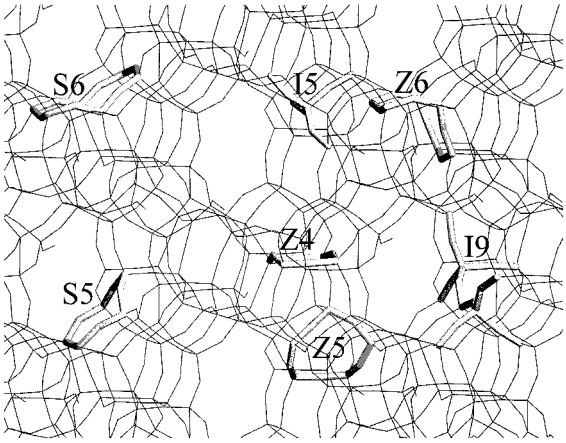

Figure 2. Location of clusters within ZSM-5 (I = intersection of straight and zigzag channels, S = straight channel, Z = zigzag channel). Arabic numerals indicate the number of T sites.

protonated form, and Figure 2 shows their location within the framework of ZSM-5.[40] The identity of the specific T sites involved in each cluster and the identity of the T sites occupied by Al are given in Table 1. For ease of referencing, each cluster is labeled as indicated in Figures 1 and 2 and Table 1. Thus, for example, S6 is a six-membered ring located in the straight channels, whereas Z6 is a six-membered ring located in the zigzag, or sinusoidal, channels. Each cluster is terminated by a H atom bonded to either an O or a Si atom located at the edge of the cluster. Either a proton or an $[M(OH)]^+$ cation is used to charge-compensate for the introduction of a single Al atom into the cluster. When two Al atoms are present in the cluster, charge compensation is done by two H^+ or two $[M(OH)]^+$ cations or by one M^{2+} or $[M-O-M]^{2+}$ cation. During the calculation, all of the atoms with the exception of the terminating H, O, and Si atoms are allowed to undergo geometric relaxation. The terminal Si−H and O−H bonds at the edge of the cluster are maintained at 1.00 and 1.50 Å, respectively.

Gradient-corrected density functional theory calculations are carried out using the B3LYP functional to estimate electron exchange and correlation contributions to the energy. Because transition metals are used for many of the clusters, numerous spin multiplicities were calculated. First, either a singlet or doublet was calculated for each cluster. Then, higher multiplicities were checked until the cluster energy increased. This procedure ensured that the lowest energy spin multiplicity was attained for each cluster. The 6-31G basis set is used to describe all atoms except the metals. For the metals, the Hay and Wadt effective core potentials and associated valence basis functions are used.[41−43] To further enhance the basis set, polarization functions are added to all atoms except for the metals and the H and O which terminate the cluster. The basis set used in the present work is identical to that used in our investigations of the stability of Cu^+ and Cu^{2+} cations in ZSM-5.[44] Bond distances and energies for CuO dimers calculated with this basis set were found to be in good agreement with those measured experimentally as well as those determined from CCSD(T) calculations.

In the acid forms of the clusters (see Figure 1), each proton can sit on one of four O atoms bound to an Al atom. All possible locations that do not lie on cluster-terminating O atoms were evaluated, and only the cluster with the lowest energy was used for further calculations. In all cases, the O−H bond distance is 0.97 Å. In rings containing two protons, the most favorable configuration is that shown in Figure 1. The positions of the protons minimize electrostatic repulsion.

Thermodynamic properties (i.e., entropy and Gibbs free energy) are estimated using standard statistical mechanical methods.[45] For gaseous species, the translational, rotational, and electronic partition functions are calculated. For a reaction involving bulk solid, such as the ZSM-5 catalyst, the translational partition functions for reactant and product clusters are taken to be equivalent because the masses of these clusters are essentially the same. The rotational partition functions for both the reactant and product clusters are taken to be unity. Because the reactant and product clusters are constrained, it is difficult to obtain reliable calculations of the vibrational partition functions for these structures. To overcome this limitation, calculations of the most relevant vibrational modes associated with each charge-exchange site were made using a small cluster containing only one T site. The estimated error in the calculated Gibbs free energies resulting from this approach is not more than ±5 kcal/mol. For the systems treated, only the ground-state degeneracy contributes to the electronic partition function.

The stability of transition-metal cations to either reduction or demetalation was evaluated by calculating the free energy of reaction for each of these processes in the following manner. For the reduction of $[M(OH)]^+$ or M^{2+}, the overall reaction is considered as the sum of two components and can be written as

$$Z^-M^{2+}(OH)^- \rightarrow Z^-H^+ + M(g) + {}^1/_2O_2(g) \quad \text{(theoretical)}$$

$$M(g) + {}^1/_2O_2(g) + H_2(g) \rightarrow M(s) + H_2O(g) \quad \text{(experimental)}$$

$$Z^-M^{2+}(OH)^- + H_2(g) \rightarrow Z^-H^+ + M(s) + H_2O(g) \quad \text{(overall)}$$

and

$$Z^-M^{2+}Z^- + H_2(g) \rightarrow Z^-H^+Z^-H^+ + M(g) \quad \text{(theoretical)}$$

$$M(g) \rightarrow M(s) \quad \text{(experimental)}$$

$$Z^-M^{2+}Z^- + H_2(g) \rightarrow Z^-H^+Z^-H^+ + M(s) \quad \text{(overall)}$$

where Z^- represents a charge-exchange site. The energy change associated with the first reaction in each set is determined theoretically, whereas the energy change associated with the second reaction is determined from experimental values.[46] One

TABLE 2: Energy of Reduction for M^{2+} Cations at I5 Sites[a]

$$Z_{I5}^{-}M^{2+}(OH)^{-} + H_2(g) \rightarrow Z_{I5}^{-}H^{+} + M(s) + H_2O(g)$$

metal	ΔE	$\Delta G°_{500K}$	metal	ΔE	$\Delta G°_{500K}$
Co	−1.6	−8.7	Pt	−112.9	−119.9
Cu	−56.0	−63.0	Rh	−86.8	−93.9
Fe	−18.9	−26.0	Ru	−91.8	−98.9
Ni	−43.8	−50.9	Zn	−0.4	−7.4
Pd	−88.8	−95.9			

[a] All energies are in kcal/mol.

of the quantities used in carrying out this latter calculation is the heat of condensation to form bulk metal. The use of bulk properties sets an upper bound on the energy change associated with the second reaction, because the magnitude of the heat of condensation for particles smaller than about 20 Å will be less than that for bulk metal.

The calculations for demetalation are handled similarly. The appropriate elementary processes are now

$$Z^{-}M^{2+}(OH)^{-} \rightarrow Z^{-}H^{+} + M(g) + {}^{1}/_{2}O_2(g) \quad \text{(theoretical)}$$

$$M(g) + {}^{x}/_{2}O_2(g) \rightarrow MO_x(s) \quad \text{(experimental)}$$

$$Z^{-}M^{2+}(OH)^{-} + {}^{(x-1)}/_{2}O_2(g) \rightarrow Z^{-}H^{+} + MO_x(s) \quad \text{(overall)}$$

and

$$Z^{-}M^{2+}Z^{-} + H_2O(g) \rightarrow Z^{-}H^{+}Z^{-}H^{+} + M(g) + {}^{1}/_{2}O_2(g) \quad \text{(theoretical)}$$

$$M(g) + {}^{x}/_{2}O_2(g) \rightarrow MO_x(s) \quad \text{(experimental)}$$

$$Z^{-}M^{2+}Z^{-} + H_2O(g) + {}^{(x-1)}/_{2}O_2(g) \rightarrow Z^{-}H^{+}Z^{-}H^{+} + MO_x(s) \quad \text{(overall)}$$

Here too, experimental values have been used to determine the heat of reaction for the second elementary process in each case, and both the metal and the metal oxide are assumed to have bulk properties.

Results and Discussion

The change in energy (ΔE) and the Gibbs free energy ($\Delta G°_{500K}$) evaluated at 500 K for reduction of an $[M(OH)]^{+}$ cation situated at an I5 site are listed in Table 2.

Reduction of the cation to zerovalent metal is favorable in all cases. The stability to H_2 reduction decreases in the order Zn > Co > Fe > Ni > Cu > Rh > Pd > Ru > Pt.

Table 3 lists values for ΔE for the reduction of M^{2+} from Z4, S5, Z5, S6, and Z6 clusters. For each metal cation, its stability to reduction depends on the structure of the cluster. Thus, Co^{2+}, Cu^{2+}, Fe^{2+}, and Ni^{2+} are most stable in S5 sites, whereas Pd^{2+}, Pt^{2+}, Ru^{2+}, and Zn^{2+} are most stable in S6 sites. By contrast, the stability of Rh^{2+} in S5, Z5, and S6 sites is approximately the same. Looking only at the sites for most stable binding, it is evident that the reduction of Co^{2+} and Zn^{2+} cations is endothermic, whereas the reduction of all other metal cations is exothermic. The stability of M^{2+} cations to reduction from rings containing two Al atoms decreases in the order Co > Zn > Fe > Ni > Cu > Ru ≈ Rh > Pd > Pt. With the exception of Rh and Ru, this is the same order as was observed for $[M(OH)]^{+}$ associated with the I5 cluster.

Comparison of the data in Tables 2 and 3 reveals that the energy for reduction of M^{2+} is almost always lower when the

TABLE 3: Energy of Reduction for M^{2+} as a Function of Charge-Exchange Site[a]

$$Z^{-}M^{2+}Z^{-} + H_2(g) \rightarrow Z^{-}H^{+}Z^{-}H^{+} + M(s)$$

metal	Z4	S5	Z5	S6	Z6
Co	NA	+4.6	NA	−6.9	NA
Cu	NA	−51.4	−57.9	−56.2	−68.9
Fe	−78.1	−6.4	−15.9	−10.1	−22.2
Ni	−125.7	−46.4	−64.4	−56.4	−58.8
Pd	−164.3	−100.2	−100.6	−91.5	−111.0
Pt	−198.4	−128.6	−132.8	−111.9	−131.6
Rh	−149.6	−93.0	−92.3	−92.2	−115.4
Ru	−151.0	−94.1	−96.1	−91.6	−122.6
Zn	−64.1	+1.2	−0.6	+2.6	−22.5

[a] All energies are in kcal/mol.

cation is exchanged as $Z^{-}M^{2+}Z^{-}$ rather than as $Z^{-}[M(OH)]^{+}$. The only exceptions to this trend are Pd^{2+} and Rh^{2+}, which favor coordination to a single Al T site in I5 over the S6 ring cluster by 2.7 and 5.4 kcal/mol, respectively.

$$Z^{-}M^{2+}(OH)^{-} + Z^{-}H^{+}Z^{-}H^{+} \rightarrow Z^{-}H^{+} + Z^{-}M^{2+}Z^{-} + H_2O(g)$$

However, when we consider the free energy of reaction that would transfer the Pd^{2+} or Rh^{2+} from the I5 to the S6 cluster, a different picture emerges. We estimate the translational and rotational entropy for water at 500 K to be 55.7 cal mol^{-1} K^{-1}. Combining this entropy and the $\Delta(PV)$ work term, we estimate the free energy to be $\Delta G_{500K} = -26.3$ kcal/mol for Pd^{2+} and $\Delta G_{500K} = -23.6$ kcal/mol for Rh^{2+}. Thus, from a free-energy standpoint metal cations uniformly prefer coordination to the S5 or S6 zeolitic ring clusters with two Al T sites over a single exchange site by a minimum of 26 kcal/mol at 500 K.

Comparison of the trends in cation reducibility reported above with experimental observations is difficult to do because the methods of cation exchange, sample pretreatment, and conditions of H_2 reduction differ from one group to another and no two groups use the same protocol. For these reasons, we have chosen to use as a criterion of reducibility the maximum temperature required to achieve complete reduction of divalent metal cations to the zerovalent metallic state during temperature-programmed reduction. This criterion is valid because temperature-programmed reactions in microporous systems occur under quasi-equilibrium conditions (see, for example, ref 47). On the basis of the maximum reduction temperature, the following sequence is obtained for the increasing ease of reduction: Zn^{2+} (>1173 K)[24,48] < Co^{2+} (993 K)[10] < Fe^{2+} (890 K)[49] < Ni^{2+} (573 K)[50] < Cu^{2+} (548 K)[21,22] < Pd^{2+} (453 K).[51] This trend is identical to that reported here for M^{2+} cations associated with I5 sites. This can be understood from a consideration of the distribution of M^{2+} cations for situations in which the M/Al ratio lies between 0.5 and 1.0, which is the case for all of the experimental situations examined. From stochastic and Monte Carlo simulations of ZSM-5 at a Si/Al ratio of 15,[52,53] the maximum value of M/Al for cations accommodated in five- and six-membered rings will be between 0.183 and 0.241, depending on whether Al in the zeolite framework is distributed thermodynamically or entirely randomly. For M/Al values larger than these limits, M^{2+} cations can be exchanged only as $Z^{-}[M(OH)]^{+}$. Thus, if the overall value of M/Al is close to unity, the majority of the M^{2+} cations will be associated with individual charge-exchange sites and not pairs of such sites. As a consequence, it is not surprising that the trend in ease of reduction is reflective of M^{2+} cations associated with isolated charge-exchange sites.

Figure 3 shows the structure of $Z_{I5}^{-}[M(OH)]^{+}$, and selected bond distances are presented in Table 4. Figure 4a illustrates

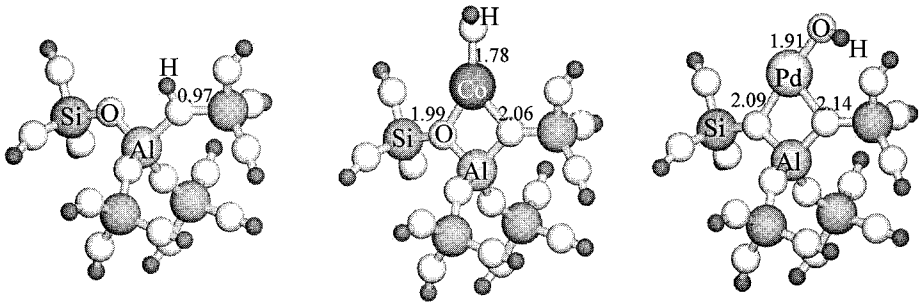

Figure 3. Structures of $Z_{I5}^{-}H^{+}$, $Z_{I5}^{-}Co^{2+}OH^{-}$, and $Z_{I5}^{-}Pd^{2+}OH^{-}$ clusters.

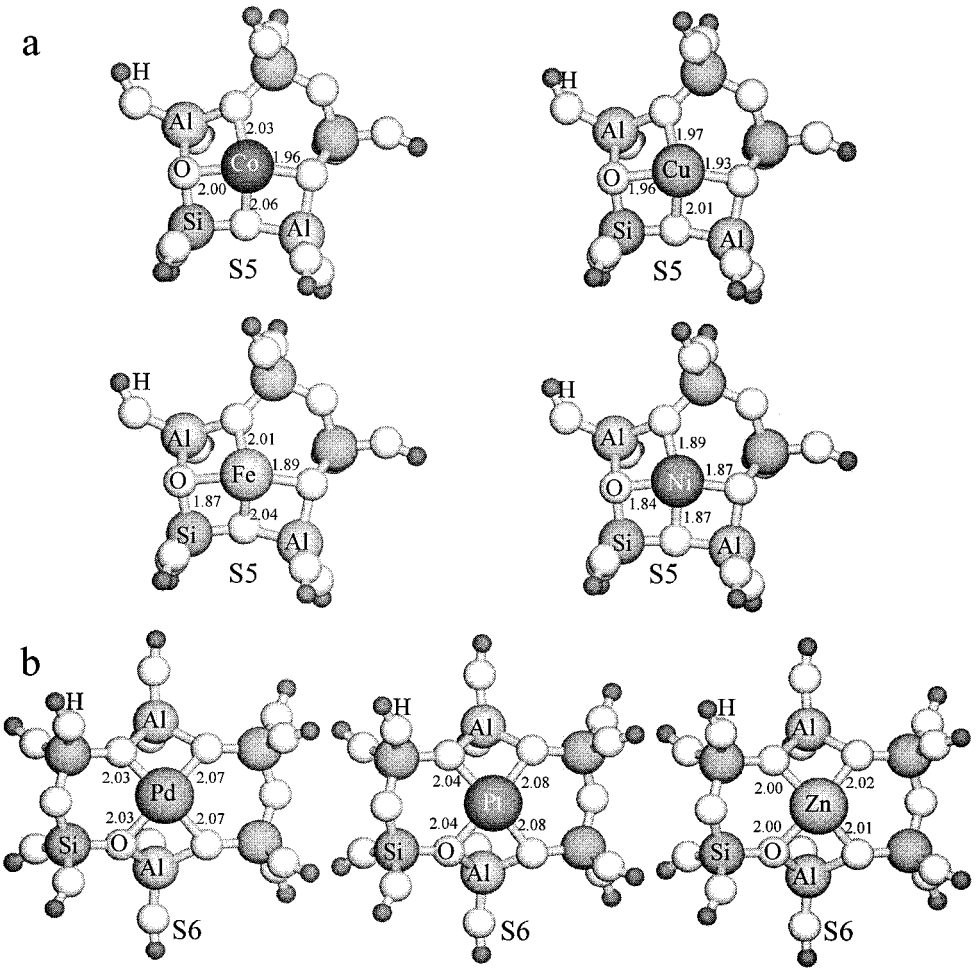

Figure 4. The geometries of (a) Co^{2+}, Cu^{2+}, Fe^{2+}, and Ni^{2+} associated with S5 sites and (b) Pd^{2+}, Pt^{2+}, and Zn^{2+} associated with S6 sites.

TABLE 4: Geometry of [$M^{2+}OH^{-}$] Associated with an I5 Site

	geometry of exchanged cluster distances (Å)			
metal cation	$(M-O_{OH})$	$(M-O_{Z1})$	$(M-O_{Z2})$	$(M-Al)$
Co	1.78	1.97	2.08	2.78
Cu	1.77	1.94	2.04	2.72
Fe	1.75	1.97	1.97	2.71
Ni	1.75	1.94	2.06	2.75
Pd	1.90	2.11	2.14	2.85
Pt	1.91	2.07	2.13	2.90
Rh	1.78	1.97	2.08	2.78
Ru	1.90	2.14	2.14	2.88
Zn	1.84	2.03	2.04	2.80

TABLE 5: Bond Distances and Angles for M^{2+} Charge-Exchanged at S5 and S6 Sites

		geometry of exchanged cluster	
metal cation	stable cluster	$(M-O)_Z$ distances (Å)	$\sum(\angle OMO)_i$ angles (deg)
Co	S5	1.97, 2.00, 2.03, 2.06	326.79
Cu	S5	1.93, 1.96, 1.97, 2.01	342.25
Fe	S5	1.89, 1.91, 1.91, 1.95	347.74
Ni	S5	1.84, 1.87, 1.87, 1.89	358.93
Pd	S6	2.03, 2.03, 2.07, 2.07	355.43
Pt	S6	2.04, 2.04, 2.08, 2.08	356.67
Rh	S6	2.04, 2.04, 2.04, 2.07	357.23
Ru	S6	2.04, 2.07, 2.07, 2.10	346.33
Zn	S6	2.00, 2.00, 2.01, 2.02	357.16

the structure for Co^{2+}, Cu^{2+}, Fe^{2+}, and Ni^{2+} situated in S5 rings, and Figure 4b illustrates the structures for Pd^{2+}, Pt^{2+}, and Zn^{2+} situated in S6 rings. Which ring type is favored depends on the length of the M−O bonds (see Table 5). For metals with an average calculated M−O bond distance of less than 2.02 Å (Co^{2+}, Cu^{2+}, Fe^{2+}, and Ni^{2+}), a five-membered ring is favored, whereas for metals with an M−O length longer than 2.03 Å (Pd^{2+}, Pt^{2+}, Rh^{2+}, Ru^{2+}, and Zn^{2+}), a six-membered ring is

TABLE 6: Energy of Demetalation for M^{2+} Cations Charge-Exchanged at I5 Sites[a]

$$Z_{I5}^{-}M^{2+}(OH)^{-} + {}^{(x-1)}/_{2}O_2(g) \rightarrow Z_{I5}^{-}H^{+} + MO_x(s)$$

metal oxide	ΔE	$\Delta G°_{500K}$	metal oxide	ΔE	$\Delta G°_{500K}$
Co_3O_4	−20.5	−15.9	Pt_3O_4	−73.8	−69.2
CuO	−41.4	−41.4	Rh_2O_3	−75.7	−64.6
Fe_2O_3	−65.3	−57.9	RuO_2	−112.6	−90.5
Ni_2O_3	−50.2	−42.8	ZnO	−31.5	−31.5
PdO	−57.1	−57.1			

[a] All energies are in kcal/mol.

preferred. How favorably a metal cation coordinates to a ring is also reflected by the sum of the four smallest angles formed by the metal cation and the four binding O atoms, $\sum(\angle OMO)_i$, listed in Table 5. The closer this sum is to 360°, the closer the metal is to a planar orientation and the better the overlap of orbitals between the metal and the four O atoms associated with the two Al atoms in the ring. If the ring is too small to accommodate the metal, as is the case for the Z4 ring, the metal cation cannot lie in the plane of the four O atoms and $\sum(\angle OMO)_i$ is significantly less than 360°. For a given ring size, visualization of the orbitals reveals that superior orbital overlap is achieved for rings in the straight channels rather than for rings in the zigzag channels.

Table 5 shows that all of the M^{2+} cations considered bind with a 4-fold coordination to the O atoms in the ring. In the S5 ring, the M−O bond distances range from 1.84 to 2.06 Å, and in the S6 ring they range from 2.01 to 2.08 Å. Comparison with experimentally reported values is difficult because determination of M−O bond distances from EXAFS data is done for samples containing M^{2+} cations in several environments. As a result, the reported M−O bond distances represent an average. Nevertheless, the agreement between calculated and observed bond distances is encouraging. Thus, for Cu−ZSM-5, Cu−O distances of 1.94[32] and 2.00 Å[54] have been reported, whereas the average calculated bond distance is 1.97 Å. In the case of Pd−ZSM-5, the reported Pd−O distance is 2.01 Å[18] and that calculated is 2.05 Å. For Zn−ZSM-5, the observed Zn−O bond distance is 2.09 Å, whereas the calculated distance is 2.01 Å.[24] Our structural predictions are similar to those reported in DFT studies of both Cu−ZSM-5 and Pd−ZSM-5. LSDA geometric structures indicate $Cu-O_{OH}$ distances of 1.76 and 1.75 Å for 1 and 5 T site models,[55] respectively. This is in close agreement with our predicted $Cu-O_{OH}$ distance of 1.77 Å.

Values of ΔE and $\Delta G°$ (500 K) for the demetalation of $[M(OH)]^+$ situated at an I5 site are listed in Table 6. From Table 6, it is evident that demetalation of $Z_{I5}^{-}[M(OH)]^+$ is favorable in all instances. The stability of the metal cations to demetalation decreases in the order Co > Zn > Cu > Ni > Pd > Fe > Rh > Pt > Ru.

Values of ΔE for demetalation of M^{2+} from rings containing two Al atoms are presented in Table 7. As in the case of reduction, Co^{2+}, Cu^{2+}, Fe^{2+}, and Ni^{2+} are most stable to demetalation when located in S5 rings, whereas Pd^{2+}, Pt^{2+}, Rh^{2+}, Ru^{2+}, and Zn^{2+} are most stable to demetalation when located in S6 rings. It is noted, though, that for Rh^{2+}, Ru^{2+}, and Zn^{2+} the stability of these cations is essentially the same in the S5 and S6 sites. The order of decreasing stability to demetalation from the site at which the M^{2+} is bound most favorably is Co > Zn > Cu > Fe ≈ Ni > Pd > Pt > Rh > Ru, which with the exception of Fe^{2+} and Rh^{2+} is the same trend seen for $[M(OH)]^{2+}$ associated with the I5 site.

The literature on the effects of O_2 and H_2O on the stability of M^{2+} cations in ZSM-5 is not sufficiently developed to enable one to identify the relative stability for a sequence of metal cations. It is clear, though, that Zn and Co are much more resistant to demetalation than Pd and that Cu has an intermediate level of stability.[6,56−58] The sequence of stability to demetalation reported here is in qualitative agreement with these observations.

TABLE 7: Energy of Demetalation for M^{2+} as a Function of Charge-Exchange Site[a]

$$Z^{-}M^{2+}Z^{-} + H_2O(g) + {}^{(x-1)}/_{2}O_2(g) \rightarrow Z^{-}H^{+}Z^{-}H^{+} + MO_x(s)$$

M_xO_y	Z4	S5	Z5	S6	Z6
Co_3O_4	NA	−14.3	NA	−25.8	NA
CuO	NA	−36.9	−43.3	−41.7	−54.4
Fe_2O_3	−124.5	−52.8	−62.3	−56.5	−68.6
Ni_2O_3	−132.1	−52.8	−70.8	−62.8	−65.2
PdO	−132.6	−68.5	−68.9	−59.7	−79.3
Pt_3O_4	−159.3	−89.4	−93.6	−72.8	−92.5
Rh_2O_3	−138.5	−81.9	−81.2	−81.1	−104.3
RuO_2	−171.8	−114.9	−116.9	−112.3	−143.4
ZnO	−95.2	−29.9	−31.7	−28.5	−53.6

[a] All energies are in kcal/mol.

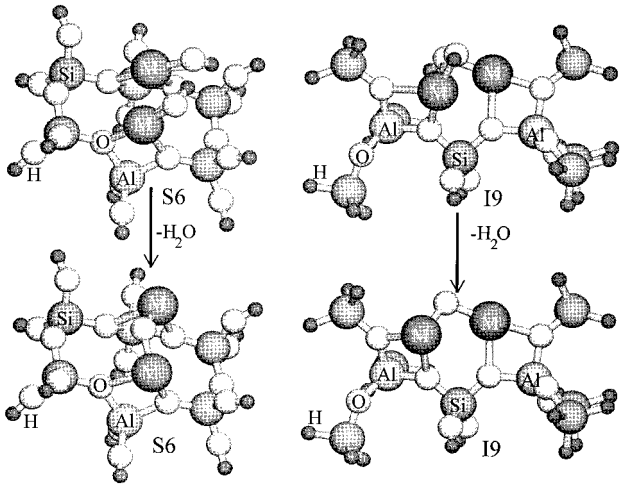

Figure 5. The structures of $[M-O-M]^{2+}$ cations associated with S6 and I9 sites.

TABLE 8: Energy of Formation for $[MOM]^{2+}$ Cations[a]

$$Z^{-}M^{2+}(OH)^{-}Z^{-}M^{2+}(OH)^{-} \rightarrow Z^{-}[MOM]^{2+}Z^{-} + H_2O(g)$$

metal	I9	S6	metal	I9	S6
Cu	+26.6	+15.6	Pd	+13.9	+29.0
Fe	+61.0	NA	Zn	+53.9	+68.4
Ni	+39.0	+25.3			

[a] All energies are in kcal/mol.

It has been proposed that metal cations can form μ-bridged metal−oxo dimers, $[M-O-M]^{2+}$.[21,22,24−28,37,30−33,36] To assess the stability of such dimers, calculations were performed for the following reaction (see Figure 5):

$$Z^{-}M^{2+}(OH)^{-}Z^{-}M^{2+}(OH)^{-} \rightarrow Z^{-}[M-O-M]^{2+}Z^{-} + H_2O$$

Table 8 lists the change in energy for this reaction for M^{2+} = Cu^{2+}, Fe^{2+}, Ni^{2+}, Pd^{2+}, and Zn^{2+}. This reaction is endothermic for all five metal cations; however, the free-energy change is favorable for Cu^{2+} and Pd^{2+} in I9 and S6 sites and for Ni^{2+} in S6 sites. For Cu and Ni, binding of the $[MOM]^{2+}$ cation is favored in an S6 ring, whereas for Pd and Zn binding of the dimer is favored in an I9 cluster. It is, therefore, evident that where $[MOM]^{2+}$ clusters are stable, their formation is driven by entropy (for T = 500 K; $T\Delta S$ = 23.9 kcal/mol) rather than by energy considerations. Consistent with the findings reported

here, evidence from EXAFS has been found for the possible existence of $[Cu-O-Cu]^{2+}$ cations.[32]

Conclusions

Divalent metal cations can be exchanged into ZSM-5 either as $[M(OH)]^+$ in association with isolated charge-exchange sites or as M^{2+} in association with a pair of charge-exchange sites that are proximate to each other. The stability to reduction of $[M(OH)]^+$ cations at I5 sites (see Table 1) via the process $Z^-M^{2+}(OH)^- + H_2(g) \rightarrow Z^-H^+ + M(s) + H_2O(g)$ decreases in the order $Zn^{2+} > Co^{2+} > Fe^{2+} > Ni^{2+} > Cu^{2+} > Rh^{2+} > Pd^{2+} > Ru^{2+} > Pt^{2+}$. This trend is good qualitative agreement with experimental observation. Co^{2+}, Cu^{2+}, Fe^{2+}, and Ni^{2+} cations are most stable in S5 sites, whereas Ru^{2+}, Pd^{2+}, Pt^{2+}, and Zn^{2+} cations are most stable in S6 sites; Rh^{2+} cations are nearly equally stable in S5, S6, and Z5 sites. The stability to reduction of M^{2+} cations from their most stable charge-exchange site via the process $Z^-M^{2+}Z^- + H_2(g) \rightarrow Z^-H^+Z^-H^+ + M(s)$ decreases in the order $Co^{2+} > Zn^{2+} > Fe^{2+} > Ni^{2+} > Cu^{2+} > Ru^{2+} = Rh^{2+} > Pd^{2+} > Pt^{2+}$. The stability of $[M(OH)]^{2+}$ cations at I5 sites to demetalation via the process $Z^-M^{2+}(OH)^- + {}^{(x-1)}/_2O_2(g) \rightarrow Z^-H^+ + MO_x(s)$ decreases in the order $Co^{2+} > Zn^{2+} > Cu^{2+} > Ni^{2+} > Pd^{2+} > Fe^{2+} > Rh^{2+} > Pt^{2+} > Ru^{2+}$. Similarly, for M^{2+} cations exchanged into their most favorable sites the stability to demetalation via the process $Z^-M^{2+}Z^- + H_2O(g) + {}^{(x-1)}/_2O_2(g) \rightarrow Z^-H^+Z^-H^+ + MO_x(s)$ decreases in the order $Co^{2+} > Zn^{2+} > Cu^{2+} > Fe^{2+} = Ni^{2+} > Pd^{2+} > Pt^{2+} > Rh^{2+} > Ru^{2+}$. The formation of μ-bridged metal−oxo dimer cations, $[M-O-M]^{2+}$, via the process $Z^-M^{2+}(OH)^-Z^-M^{2+}(OH)^- \rightarrow Z^-[M-O-M]^{2+}Z^- + H_2O$ is endothermic for Cu^{2+}, Fe^{2+}, Ni^{2+}, and Pd^{2+}. However, the free-energy change for this process is favorable for Cu^{2+} and Pd^{2+} in I9 and S6 sites and for Ni^{2+} in S6 sites. Finally, it must be recognized that the relative stability of metal cations having comparable stability could be affected by a change in the basis set used for the calculations.

Acknowledgment. This work was supported by the Director, Office of Energy Science, Chemical Sciences Division, of the U.S. Department of Energy under Contract DE-AC03-SF7600098. Computational resources were provided by the National Energy Research Supercomputer Center.

References and Notes

(1) Iwamoto, M.; Yoke, S.; Sakai, K.; Kagawa, S. *J. Chem. Soc., Faraday Trans.* **1981**, *77*, 1629.
(2) Iwamoto, M.; Furukawa, H.; Kagawa, S. *New Developments in Zeolite Science and Technology*; Murukama, Y., Ichijima, A., Ward, J. W., Eds.; Elsevier: Amsterdam, 1986; p 943.
(3) Iwamoto, M.; Hamada, H. *Catal. Today* **1991**, *10*, 57.
(4) Iwamoto, M.; Yahiro, H.; Tanada, K.; Mozino, Y.; Mine, Y.; Kagawa, S. *J. Phys. Chem.* **1991**, *95*, 3727.
(5) Zhang, Y.; Flytzani-Stephanopoulos, M. Catalytic Decomposition of Nitric Oxide over Promoted Copper-Ion-Exchanged ZSM-5 Zeolites. In *Environmental Catalysis*; Armor, J. N., Ed.; ACS Symposium Series 552; American Chemical Society: Washington, DC, 1994; p 7.
(6) Li, Y.; Armor, J. N. *Appl. Catal. B* **1992**, *1*, L21.
(7) Armor, J. N.; Farris, T. S. *Appl. Catal., B* **1994,** *4*, L11.
(8) Chang. Y. F.; McCarty, J. G.; Wachsman, E. D.; Wong, V. L. *Appl. Catal., B* **1994**, *4*, 283.
(9) Kapteijn, F.; Rodriguez-Mirasol, J.; Moulijn, J. A. *Appl. Catal., B* **1996**, *9*, 25.
(10) da Cruz, R. S.; Mascarenhas, A. J. S.; Andrade, H. M. C. *Appl. Catal., A* **1998**, *18*, 223.
(11) Li, Y.; Armor, J. N. *Appl. Catal., B* **1992**, *1*, L31.
(12) Li, Y.; Armor, J. N. *Appl. Catal., B* **1993**, *2*, 239.
(13) Shelef, M. *Chem. Rev.* **1995**, *95*, 209.
(14) Loughran, C. J.; Resasco, D. E. *Appl. Catal., B* **1995**, *7*, 113.
(15) Misono, M.; Hirao, Y.; Yokoyama, C. *Catal. Today* **1997**, *38*, 157.
(16) Ogura, M.; Hayaskhi, M.; Kikuchi, E. *Catal. Today* **1998**, *45*, 139.
(17) Ogura, M.; Sugiura, Y.; Hayaskhi, M.; Kikuchi, E. *Catal. Lett.* **1996**, *42*, 185.
(18) Ali, A.; Alvarez, W.; Loughran, C. J.; Resasco, D. E. *Appl. Catal., B* **1997**, *14*, 13.
(19) Feng, X.; Hall, W. K. *J. Catal.* **1997**, *166*, 368.
(20) Xin, M.; Hwang, I. C.; Kim, D. H.; Cho, S. I.; Woo, S. I. *Appl. Catal., B* **1999**, *21*, 183.
(21) Voskoboinikov, T. V.; Chen, H. Y.; Sachtler, W. M. H. *Appl. Catal., B* **1998,** *19*, 279.
(22) Yan, J. Y.; Sachtler, W. M. H.; Kung, H. H. *Catal. Today* **1997**, *33*, 279.
(23) Biscardi, J. A.; Iglesia, E. *Catal. Today* **1996**, *31*, 207.
(24) Biscardi, J. A.; Meitzner, G. D.; Iglesia, E. *J. Catal.* **1998**, *179*, 192.
(25) Hamada, H.; Matsubayashi, N.; Shimada, H.; Kintaichi, Y.; Ito, T.; Nishijima, A. *Catal. Lett.* **1990**, *5*, 189.
(26) Iwamoto, M.; Yahiro, H.; Tanada, K.; Mizuno, N.; Mine, Y.; Kagawa, S. *J. Phys. Chem.* **1991**, *95*, 3727.
(27) Zhang, Z.; Lerner, B.; Lei, G.-D.; Sachtler, W. M. H. *J. Catal.* **1993**, *140*, 481.
(28) Sarkany, J.; d'Itri, J. L.; Sachtler, W. H. M. *Catal. Lett.* **1992**, *16*, 241.
(29) Campa, M. C.; Indovina, V.; Minelli, G.; Pettiti, I.; Riccio, A. *Catal. Lett.* **1994**, *23*, 141.
(30) Moretti, G. *Catal. Lett.* **1994**, *23*, 135.
(31) Moretti, G. *Catal. Lett.* **1994**, *28*, 143.
(32) Grünert, W.; Hayes, N. W.; Joyner, R. W.; Shpiro, E. S.; Siddiqui, M. R. H.; Baeva, G. N. *J. Phys. Chem.* **1994**, *98*, 10832.
(33) Feng, X.; Hall, W. K. *Catal. Lett.* **1997**, *46*, 11.
(34) Kuroda, Y.; Kumashiro, R.; Yoshimoto, T.; Nagao, M. *Phys. Chem. Chem. Phys.* **1999**, *1*, 649.
(35) Marturano, P.; Drozdová, L.; Kogelbauer, A.; Prins, R. *J. Catal.* **2000**, *192*, 236.
(36) Zhang, Z.; Lerner, B.; Lei, G.-D.; Sachtler, W. M. H. *J. Catal.* **1993**, *140*, 481.
(37) Yan, J. Y.; Lei, G.-D.; Sachtler, W. M. H.; Kung, H. H. *J. Catal.* **1996,** *161*, 43.
(38) Goodman, B. R.; Schneider, W. F.; Hass, K. C.; Adams, J. B. *Catal. Lett.* **1998**, *56*, 183.
(39) Goodman, B. R.; Hass, K. C.; Schneider, W. F.; Adams, J. B. *J. Phys. Chem. B* **1999**, *103*, 10452.
(40) Olson, D. H.; Kokotallo, G. T.; Lawton, S. L.; Meier, W. M. *J. Phys. Chem.* **1981**, *85*, 2238.
(41) Hay, P. J.; Wadt, W. R. *J. Chem. Phys.* **1985**, *82*, 270.
(42) Hay, P. J.; Wadt, W. R. *J. Chem. Phys.* **1985**, *82*, 284.
(43) Hay, P. J.; Wadt, W. R. *J. Chem. Phys.* **1985**, *82*, 299.
(44) Rice, M. J.; Chakraborty, A. K.; Bell, A. T. *J. Phys. Chem. A* **1998**, *102*, 7498.
(45) McQuarrie, D. A. *Statistical Mechanics*; HarperCollins Publisher Inc.: New York, 1973.
(46) *CRC Handbook of Chemistry and Physics*, 61st ed.; Weast, R. C., Astle, M. J., Eds.; CRC Press: Boca Raton, FL, 1980.
(47) Riek, J. S.; Bell, A. T. *J. Catal.* **1984**, *85*, 143.
(48) El-Malki, E. M.; van Santen, R. A.; Sachtler, W. M. H. *J. Phys. Chem. B* **1999**, *103*, 4611.
(49) Lobree, L. J.; Hwang, I.-C.; Reimer, J. A.; Bell, A. T. *J. Catal.* **1999**, *186*, 242.
(50) Jentys, A.; Lugstein, A.; Vinek, H. *Zeolites* **1997**, *18*, 391.
(51) Cañizares, P.; DeLucas, A.; Valverde, J. L.; Dorado, F. *Ind. Eng. Chem. Res.* **1998**, *37*, 2592.
(52) Rice, M. J.; Chakraborty, A. K.; Bell, A. T. *J. Catal.* **1999**, *186*, 222.
(53) Rice, M. J.; Chakraborty, A. K.; Bell, A. T. *J. Catal.*, in press.
(54) Yamashita, H.; Matsuoka, M.; Tsuji, K.; Shioya, Y.; Anpo, M.; Che, M. *J. Phys. Chem.* **1996**, *100*, 397.
(55) Hass, K. C.; Schneider, W. F. *Phys. Chem. Chem. Phys.* **1999**, *1*, 639.
(56) Li, Y.; Armor, J. N. *Appl. Catal., B* **1997**, *3*, 275.
(57) Li, Y. J.; Battavio, P. J.; Armor, J. N. *J. Catal.* **1993**, *142*, 561.
(58) Lee, J. K.; Lee, H. T.; Rhee, H. K. *React. Kinet. Catal. Lett.* **1996**, *57*, 323.